JOC*Article*

Exohedral Reactivity of Trimetallic Nitride Template (TNT) Endohedral Metallofullerenes

Josep M. Campanera,[‡] Carles Bo,[‡] and Josep M. Poblet*[,†]

Departament de Química Física i Inorgànica, Universitat Rovira i Virgili, c/Marcel lí Domingo, s/n, Campus Sescelades, 43007 Tarragona, Catalonia, Spain, and ICIQ−Institut Català d'Investigació Química, Avda. Països Catalans, 16, 43007 Tarragona, Catalonia, Spain

josepmaria.poblet@urv.net

Received August 8, 2005

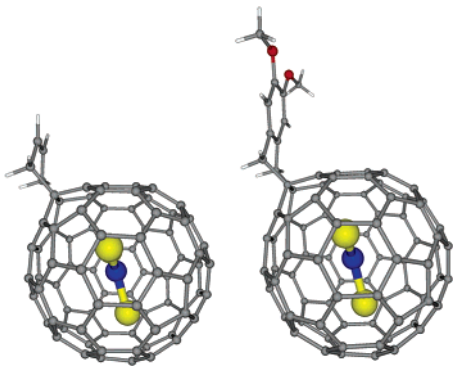

Fullerenes containing a trimetallic nitride template (TNT) within the cage are a particularly interesting class of endohedral metallofullerenes. Recently two exohedral derivatives of the $Sc_3N@C_{80}$ fullerene have been synthesized: a Diels−Alder and a fulleropyrrolidine cycloadduct. The successful isolation, purification, and structural elucidation of these metallofullerenes derivatives have encouraged us to understand how the chemical reactivity is affected by TNT encapsulation. First of all, we predicted the most reactive exohedral sites, taking into account the double bond character and the pyramidalization angle of the C−C bonds. For this purpose, a full characterization of all different types of C−C bonds of the following fullerenes was carried out: I_h-C_{60}:**1**, D_3-C_{68}:**6140**, D_3-$Sc_3N@C_{68}$, D_{5h}-C_{70}:**1**, $D_{3h'}$-C_{78}:**5**, D_{3h}-$Sc_3N@C_{78}$, I_h-C_{80}:**7** and several isomers of $Sc_3N@C_{80}$. Finally the exohedral reactivity of these TNT endohedral metallofullerenes, via [4 + 2] cycloaddition reactions of 1,3-butadiene, was corroborated by means of DFT calculations.

Introduction

Many fullerenes with encapsulated metals and nonmetals have been reported, but they are typically formed in low yields (<0.5%) that have prevented progress in the exploration of their chemical and physical properties.[1] However, a new family of trimetallic nitride template (TNT) endohedral metallofullerenes has been reported recently in relatively higher yields with a general formula of $A_{3-n}B_nN@C_k$ ($n = 0-3$; A, B = group III, IV, and rare-earth metals; $k = 68, 78, 80$). The archetypal examples, in chronological order of their first reported synthesis, are $Sc_3N@C_{80}$,[2] $Sc_3N@C_{68}$,[3] and $Sc_3N@C_{78}$[4] (Figure 1). In these, not only are the cage properties modified by the presence of the incarcerated group but, almost uniquely among endohedral metallofullerenes, they are quite stable. Furthermore, they can be produced in multimilligram quantities, and these amounts should increase in the future. The electronic effect of the TNT

[†] Universitat Rovira i Virgili.
[‡] ICIQ−Institut Català d'Investigació Química.

(1) Akasaka, T.; Nagase, S. *Endofullerenes: A New Family of Carbon Clusters, Developments in Fullerene Science*; Kluwer Academic Publishers: Dordrecht, 2002.

(2) Stevenson, S.; Rice, G.; Glass, T.; Harich, K.; Cromer, F.; Jordan, M. R.; Craft, J.; Hadju, E.; Bible, R.; Olmstead, M. M.; Maltra, K.; Fisher, A. J.; Balch, A. L.; Dorn, H. C. *Nature* **1999**, *401*, 55.

(3) Stevenson, S.; Fowler, P. W.; Heine, T.; Duchamps, J. C.; Rice, G.; Glass, T.; Harich, K.; Hajdu, E.; Bible, R.; Dorn, H. C. *Nature* **2000**, *408*, 428.

(4) Olmstead, M. M.; Bettencourt-Dias, A.; Duchamp J. C.; Stevenson, S.; Marciu, D.; Dorn, H. C.; Balch, A. L. *Angew. Chem., Int. Ed.* **2001**, *40*, 1223.

10.1021/jo051665s CCC: $33.50
Published on Web 11/23/2005

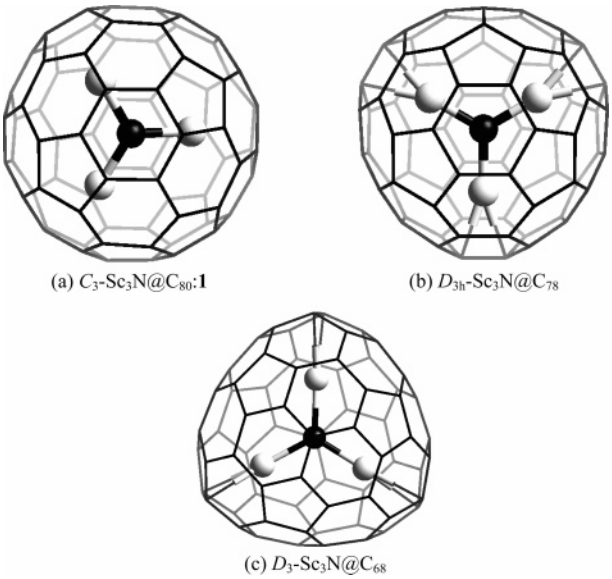

FIGURE 1. Optimized structures.

group is such that some fullerenes of sizes and symmetry that are otherwise relatively unstable become available for investigation.[5]

TNT endohedral metallofullerenes have also attracted special attention because they engender new spherical molecules with unique electronic properties and structures that are unexpected for empty fullerenes. It would be of interest to understand how the exohedral chemical functionalization is affected by the endohedral metal-doping. Experiments have shown a remarkable regioselectivity of the addition and cycloaddition reactions to I_h-C_{60}:**1** and D_{5h}-C_{70}:**1**, which occur to the 6:6 pyracylene C−C bonds in C_{60} and to the 6:6 pyracylene Ca−Cb/Cc−Cc in the C_{70}.[6] Theoretical studies of these cycloaddition reactions, from the kinetic and thermodynamic point of view, have also corroborated the high regioselectivity.[7] These results encouraged us to find out how much the exohedral regioselectivity of the D_3-C_{68}:**6140**, $D_{3h'}$-C_{78}:**5**, and I_h-C_{80}:**7** free cages changes after the TNT encapsulation. The new electronic structure imposed by the TNT encapsulation is the first to take into account. The bonding of the TNT endohedral metallofullerenes is widely described by the ionic model $Sc_3N^{6+}@C_k^{6-}$, and thus the six

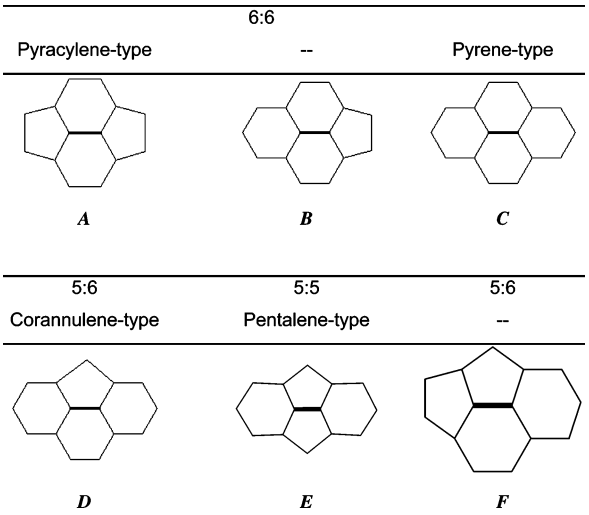

FIGURE 2. All different types of C−C bonds in IPR fullerenes (***A***−***D*** types) and two additional types found in the non-IPR D_3-C_{68}:**6140** isomer (***E*** and ***F*** types). The bold line determines the C−C bond considered. The 6:6 ring junction in the ***A*** type is abutted by two pentagons (pyracylene-type site), by a hexagon and a pentagon in the ***B*** type, and by two hexagons in the ***C*** type (pyrene-type site). The ***D*** type is called a corannulene-type site and represents a 5:6 ring junction abutted by two hexagons. The ***E*** type, called a pentalene-type site, is a 5:5 ring junction abutted by two hexagons, and the ***F*** type is a 5:6 ring junction abutted by a pentagon and a hexagon. The two last types (the ***E*** and ***F***) are very destabilizing and only found in non-IPR fullerenes.

electron transfer from the TNT unit to the cage will change the electronic structure of the cage. As far as exohedral reactivity is concerned, two characteristics appear to be determinant in the cycloaddition reactions. First, regardless of the bond type, short bond lengths (which mean larger π-bond orders and higher π-density) are preferred, and second, additions to pyramidalized C−C bonds are favored.[7] Consequently a complete description of all different types of C−C bonds is necessary to search the most reactive sites. This description is collated in Supporting Information, Tables A.1−A.5 and Figures A.1−A.5, for I_h-C_{60}:**1**, D_3-C_{68}:**6140**, D_{5h}-C_{70}:**1**, $D_{3h'}$-C_{78}:**5**, and I_h-C_{80}:**7**. The description includes bond lengths, pyramidalization angles, and bond orders. Motifs of all possible types of C−C bonds of the IPR fullerenes (***A***−***D*** types) and two C−C bonds of the non-IPR fullerenes (***E***, ***F***) are described in Figure 2. In general, each motif is described by a specific range of bond lengths, pyramidalization angles, and bond orders, which characterize and differentiate them.

Classical endohedral metallofullerenes were the first to be exohedrally functionalized. The $La_2@C_{80}$ and $Sc_2@C_{84}$ dimetallofullerenes were functionalized by thermal and photochemical reactions with an excess of 1,1,2,2-tetramesityl-1,2-disilirane to give the $La_2@C_{80}$-$(Mes_2Si)_2CH_2$ and $Sc_2@C_{84}$-$(Mes_2Si)_2CH_2$ adducts, respectively.[8] The analogous exohedral derivative of $La@C_{82}$, $La@C_{82}(Mes_2Si)_2CH_2$, was also synthesized. Unlike the first two exohedral compounds, this compound provided the additional valuable information that no multiple addition occurred.[9] A carbene derivative of this monometallofullerene,

(5) (a) Aihara, J. *J. Phys. Chem. A* **2002**, *106*, 11371. (b) Nagase, S.; Kobayashi, K.; Akasaka, T. *J. Mol. Struct. (THEOCHEM)* **1999**, *461*, 97. (c) Kobayashi, K.; Nagase, S.; Yoshida, M.; Osawa, E. *J. Am. Chem. Soc.* **1997**, *119*, 12693. (d) Slanina, Z.; Ishimura, K.; Kobayashi, K.; Nagase, S. *Chem. Phys. Lett.* **2004**, *384*, 114. (e) Kato, H.; Taninaka, A.; Sugai, T.; Shinohara, H. *J. Am. Chem. Soc.* **2003**, *125*, 7782. (f) Nagase, S.; Kobayashi, K. *Chem. Phys. Lett.* **1997**, *276*, 55. (g) Wang, C.; Kai, T.; Tomiyama, T.; Yoshida, T.; Kobayashi, Y.; Nishibori, E.; Takata, M.; Sakata, M.; Shinohara, H. *Nature* **2000**, *408*, 426.

(6) (a) Tsuda, M.; Ishida, T.; Nogami, T.; Kurono S.; Ohashi, M. *J. Chem. Soc., Chem. Commun.* **1993**, 1296. (b) Meidine, M. F.; Roers, R.; Langley, G. J.; Avent, A. G.; Darwish, A. D.; Firth, S.; Kroto, H. W.; Taylor, R.; Walton, D. R. M. *J. Chem. Soc., Chem. Commun.* **1993**, 1342. (c) Liu, S.; Lu, Y.; Kappas, M. M.; Ibers, J. A. *Science* **1991**, *254*, 410. (d) Rubin, Y.; Kahn, S. I.; Freeberg, D. I.; Yeretzian, C. *J. Am. Chem. Soc.* **1993**, *115*, 344. (e) Pang, L. S. K.; Wilson, M. A. *J. Phys. Chem.* **1993**, *97*, 6761. (f) Kräutler, B.; Maynollo, J. *Angew. Chem., Int. Ed. Engl.* **1995**, *34*, 87. (g) Lamparth, I.; Maichle-Mössmer, C.; Hirsch, A. *Angew. Chem., Int. Ed. Engl.* **1995**, *34*, 1607.

(7) Solà, M.; Duran, M.; Mestres, J. *J. Am. Chem. Soc.* **1996**, *118*, 8920. (b) Mestres, J.; Duran, M.; Solà, M. *J. Phys. Chem.* **1996**, *100*, 7449. (c) Mestres, J.; Solà, M. *J. Org. Chem.* **1998**, *63*, 7556. (d) Chikama, A.; Fueno, H.; Fujimoto, H. *J. Phys. Chem.* **1995**, *99*, 8541.

(8) Akasaka, T.; Nagase, S.; Kobayashi, K.; Suzuki, T.; Kato, T.; Kikuchi, K.; Achiba, Y.; Yamamoto, K.; Funasaka, H.; Takahashi, T. *Angew. Chem., Int. Ed. Engl.* **1995**, *34*, 19.

(9) Takeshi, A.; Kato, T.; Kobayashi, K.; Nagase, S.; Yamamoto, K.; Funasaka, H.; Takahashi, T. *Nature* **1995**, *374*, 600.

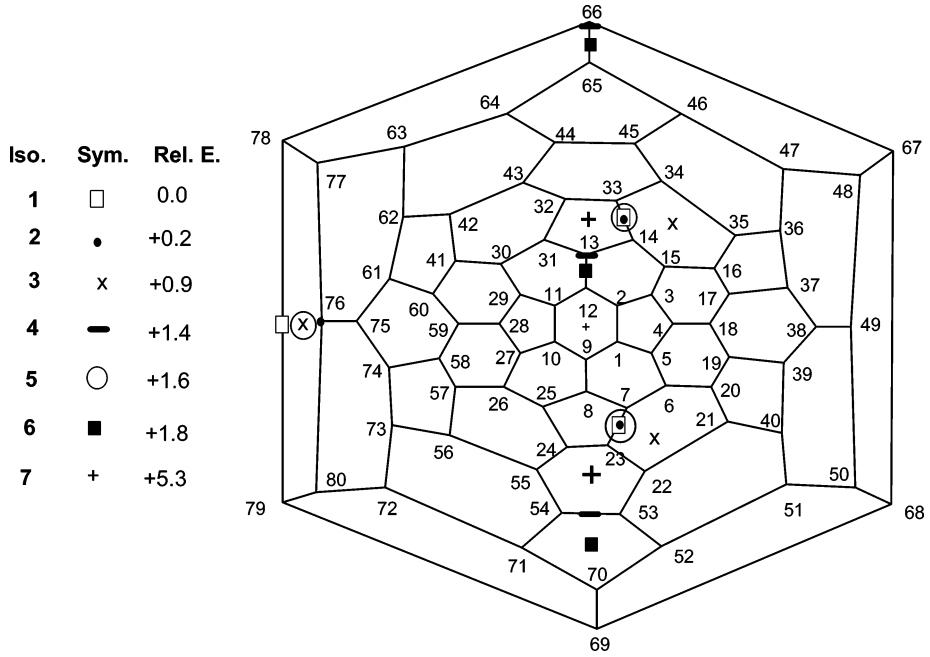

FIGURE 3. Schlegel diagram of I_h-C_{80}:**7** with the six isomers of $Sc_3N@C_{80}$:**1**−**7** and their relative energies in kcal mol^{-1}. The symbols represent the position where scandiums are facing endohedrally the fullerene cage.

$La@C_{82}$, has also been reported recently.[10] Kobayashi and co-workers carried out density functional calculations for two $La_2@C_{80}$ derivatives, $La_2@C_{80}$-($C_8H_6(OCH_3)_2$) and $La_2@C_{80}$-($Si_2H_4CH_2$).[11] They concluded that the attachment of the electron-accepting molecule $C_8H_6(OCH_3)_2$ has no significant effect on the internal rotation in $La_2@C_{80}$, but the random circular motion of two La atoms in $La_2@C_{80}$ could be highly controlled by attaching exohedrally electron-donating molecules such as disilirane (*c*-$Si_2R_4CH_2$). The 1,4-cycloaddition is the most favorable for the disilirane additions, whereas the 1,2-cycloaddtion in the 5:6 C−C bond of I_h-C_{80}:**7** occurs for Diels−Alder compounds.

Dorn and co-workers have proposed a structure for the first symmetric derivative of the TNT endohedral metallofullerene of I_h-C_{80}:**7** (Figure 1a) formed when it reacts with the 6,7-dimetoxyisochroman-3-one diene precursor.[12,13] The final structure is a Diels−Alder cycloadduct, $Sc_3N@C_{80}$-$C_8H_6(OCH_3)_2$, which is produced via a [4 + 2] cycloaddition mechanistic pathway.[14] The $Sc_3N@C_{80}$ acts as an electron-deficient dienophile and the 6,7-dimetoxyisochroman-3-one as a diene precursor. The product has been crystallographically characterized, and the ^{13}C NMR suggested that the molecule possesses a plane of symmetry.[15] Unlike C_{60}, the I_h-C_{80}:**7** cage does not have any of the reactive 6:6 pyracylene C−C bonds (***A*** type). Instead of that C−C bond, the I_h-C_{80}:**7** cage contains only corannulene 5:6 C−C bonds (***D*** type) and C−C bonds at 6:6 ring junctions abutted by a hexagon and a pentagon (***B*** type), Figure 2. The cycloaddition occurs specifically to the 5:6 C1−C2 bond, which is elongated and pulled away from the center of the carbon cage toward the addend.[16] Moreover, a detailed inspection of the geometry shows that the Sc_3N unit is positioned well away from the site of external modification, in a relative position corresponding to that of the $Sc_3N@C_{80}$:**2** isomer. Recently, the 1,3-dipolar cycloaddition of the *N*-ethylazomethine ylide also on the 5:6 C1−C2 bond on the surface of the $Sc_3N@C_{80}$:**2** isomer has been reported.[17] However, we cannot only focus our study on the 5:6 C−C bonds, because the same cycloaddition of N-ethylazomethine ylide on $Y_3N@C_{80}$ yielded mainly the pyrrolidine monoadduct exclusively at a 6:6 C−C bond and thus the exohedral reactivity seems to be dictated by the encapsulated metal cluster.[18] As regards to the several orientations of the TNT unit, in the $Sc_3N@C_{80}$ we corroborated that the encapsulated nitride is not located at any specific internal bonding site and consequently the TNT unit may freely rotate inside the cage (Figure 1a).[19] Six isomers of $Sc_3N@C_{80}$:**1**−**6**[20] (Figure 3) were studied theoretically and the differences among the most stable isomers are rather small, 0−2 kcal mol^{-1}. Several different orientations of the TNT have been found experimentally for the slightly different TNT endohedral metallofullerenes of I_h-C_{80}:**7**, $ErSc_2N@C_{80}$ (isomer **4**)[21] and

(10) Maeda, Y.; Matsunaga, Y.; Wakahara, T.; Takahashi, S.; Tsuchiya, T.; Ishitsuka, O.; Hasegawa, T.; Akasaka, T.; Liu, M. T. H.; Kokura, K.; Horn, E.; Yoza, K.; Kato, T.; Okubo, S.; Kobayashi, K.; Nagase, S.; Yamamoto, K. *J. Am. Chem. Soc.* **2004**, *126*, 6858.

(11) Kobayashi, K.; Nagase, S.; Maeda, Y.; Wakahara, T.; Akasaka, T. *Chem. Phys. Lett.* **2003**, *374*, 562.

(12) Iezzi, E. B.; Ducamp, J. C.; Harich, K.; Glass, T. E.; Lee, H. M.; Olmstead, M. M.; Balch, A. L.; Dorn, H. C. *J. Am. Chem. Soc.* **2002**, *124*, 524.

(13) A minor isomer corresponding to the Sc_3N encapsulation inside the D_{5h}-C_{80}:**6** isomer has also been found, although no indication of exohedral functionalization has yet been reported.

(14) (a) Belik, P.; Gügel, A.; Kraus, A.; Spickermann, J.; Enkelmann, V.; Frank, G.; Müllen, K. *Adv. Mater.* **1993**, *5*, 854. (b) Belik, P.; Gügel, A.; Kraus, A.; Spickermann, J.; Enkelmann, V.; Frank, G.; Müllen, K. *Angew. Chem., Int. Ed. Engl.* **1993**, *32*, 78.

(15) Lee, H. M.; Olmstead, M. M.; Iezzi, E.; Duchamp, J. C.; Dorn, H. C.; Balch, A. L. *J. Am. Chem. Soc.* **2002**, *124*, 3494.

(16) The systematic numbering system was taken from Taylor, R. *J. Chem. Soc., Perkin Trans. 2* **1993**, 813.

(17) Cardona, C. M.; Kitaygorodskiy, A.; Ortiz, A.; Herranz, A.; Echegoyen, L. *J. Org. Chem.* **2005**, *70*, 5092.

(18) Cardona, C. M.; Kitaygorodskiy, A.; Echegoyen, L. *J. Am. Chem. Soc.* **2005**, *127*, 10448.

(19) Campanera, J. M.; Bo, C.; Olmstead, M. M.; Balch, A. L.; Poblet, J. M. *J. Phys. Chem. A.* **2002**, *106*, 12356.

(20) The numbering of the isomers is different in ref 19. Isomers **1**, **2**, **3**, **4**, **5**, **6**, and **7** in this article correspond to **11**, **12**, **10**, **7**, **9**, **8**, and **6**, respectively, in the old reference.

$Sc_3N@C_{80}$ (isomer **1**).[2,22] The isomers $Sc_3N@C_{80}$:**1** and **2** are predicted to be almost isoenergetic, the former being favored by a mere 0.2 kcal mol^{-1}. The slight difference consists only in the position of one Sc atom: in the former it faces a 5:6 C−C bond and in the later it faces a single carbon atom.

Dorn and co-workers derivatized also the $Sc_3N@C_{78}$ with a ^{13}C-labeled reagent and obtained mono-, di-, and triadducts.[23] The ^{13}C and ^1H NMR data of the monoadduct support the idea that addend addition takes place at an asymmetric site on the $D_{3h'}$-C_{78}:**5** cage. Unlike the $Sc_3N@C_{80}$, the scandium ions are strongly linked to the pyracylene 6:6 C−C bonds (Figure 1b). This bond does not allow the Sc_3N unit to rotate freely inside the fullerene, and consequently only one isomer is possible.[19] The fourth fullerene cage that is capable of incarcerating four atoms is the non-IPR D_3-C_{68}:**6140**, Figure 1c.[24] However, this TNT endohedral metallofullerene has not yet been exohedral functionalized.

The aim of this work is to answer two main questions: (1) How does the encapsulation of a TNT unit affect the exohedral reactivity of these TNT endohedral metallofullerenes, especially on $Sc_3N@C_{80}$? (2) Which are the most reactive sites toward cycloadditon reaction of 1,3-butadiene in the free I_h-C_{80}:**7** cage and in the $Sc_3N@C_{80}$ isomers (**1**, **2**, and **7**)? This thermodynamic study also comprises some clues about the exohedral reactivity of the free fullerenes $D_{3h'}$-C_{78}:**5** and D_3-C_{68}:**6140** and their corresponding TNT endohedral fullerenes. We have rationalized the preferred sites for the nucleophilic attack on the basis of the strength of the C−C bonds (bond orders and bond lengths) and pyramidalization angles of carbons.

Computational Details

Geometry optimizations were carried out using the DFT methodology with the ADF2004 program.[25] The local density approximation (LDA) characterized by the electron-gas exchange together with the Vosko−Wilk−Nusair[26] (VWN) parametrization for correlation was used. Becke [27] and Perdew [28] nonlocal corrections were added to the exchange and correlation energy, respectively. First-order Pauli scalar relativistic corrections were added variationally to the total energy for all systems. Triple-ζ polarization Slater basis sets were employed to describe the valence electrons of C, Sc, and N. A frozen core consisting of the 1s shell was described by means of single Slater functions for C and N. A frozen core composed of the 1s to 2sp shells for Sc was described by means of single Slater functions. The 3s and 3p electrons were described by double-ζ Slater functions, the *n*d and $(n + 1)$s electrons by triple-ζ functions, and the $(n+1)$p electrons by a single orbital.[29]

Bond indices were obtained according to Mayer's definition, with a program[30] designed for their calculation from the ADF output file. Pyramidalization angles (θ_p) have been calculated using the π-orbital axis vector approach (POAV1)[31] as implemented in the MOL2MOL program.[32]

Results and Discussion

Effects of TNT Encapsulation on the Exohedral Reactivity. It is well-known that fullerenes can accept electrons and, thus, prefer to react with electron-rich reagents.[33] Moreover, Diels−Alder reactions are facilitated by electron-withdrawing dienophiles. So the comparison of the electron affinity between the free cage and the TNT endohedral metallofullerene will be determinant in order to establish the electronic effect of the TNT encapsulation on the final reactivity. On the other hand, we also consider the geometric effect of the TNT encapsulation to the double bond character and pyramidalization of C−C bonds, which will help us to find the most reactive sites. In regards to this consideration, the C−C bond of the dienophile must be markedly of double bond character and pyramidalized.

Electronic Effect: Electron−Attracting Character. The electronic structure of I_h-C_{80}:**7** was characterized by the presence of energetically low-lying 4-fold degenerate LUMOs, which enables this fullerene to accept up to six electrons. This is corroborated by a high electron affinity (EA) of 3.75 eV. After the TNT endohedral doping, the EA of the new molecule decreases to 2.99 eV for the $Sc_3N@C_{80}$:**1** isomer.[19] Although data are only available for the $Sc_3N@C_{80}$:**1** isomer, it is expected that the encapsulation process will modify the EA in the same way for all isomers of $Sc_3N@C_{80}$. This completely agrees with the experimental value of 2.81 ± 0.05 eV estimated by Ioffe et al.[34] The electronic behavior of the TNT endohedral doping differs from that of the classical endohedral metallofullerenes such as $M_n@C_k$ (M = Sc, Y, La, Gd; $n = 1, 2$). The EAs of the mono- and dimetallofullerenes are higher than those of the corresponding free fullerenes.[34] As an example, the first EA determination for a metallofullerene was performed in 1992, and electron affinity of $Ca@C_{60}$ estimated from the threshold of the photoelectron spectrum was found to be about 3.0 eV, which is 0.3 eV higher than that for C_{60}.[35] In relation, recently, Nagase and co-workers confirmed that $Sc_3N@C_{80}$ has a much lower thermal reactivity toward disilirane than $La_2@C_{80}$, though these two metallofullerenes have the same electronic structure

(21) Olmstead, M. M.; Bettencourt-Dias, A.; Duchamp, J. C.; Stevenson, S.; Dorn, H. C.; Balch, A. L. *J. Am. Chem. Soc.* **2000**, *122*, 12220.
(22) Stevenson, S.; Lee, H. M.; Olmstead, M. M.; Kozikowski, C.; Stevenson, P.; Balch, A. L. *Chem. Eur. J.* **2002**, *8*, 4528.
(23) Iezzi, E. B. Ph.D. Dissertation, Virgina Tech, 2003.
(24) (a) Stevenson, S.; Fowler, P. W.; Heine, T.; Duchamp, J. C.; Rice, G.; Glass, T.; Harich, K.; Hajdu, E.; Bible, R.; Dorn, H. C. *Nature* **2000**, *408*, 428. (b) Olmstead, M. M.; Lee, H. M.; Duchamp, J. C.; Stevenson, S.; Marciu, D.; Dorn, H. C.; Balch, A. L. *Angew. Chem., Int. Ed.* **2003**, *42*, 900.
(25) (a) ADF2004.01, SCM, Theoretical Chemistry, Vrije Universiteit, Amsterdam, The Netherlands, http://www.scm.com. te Velde, G.; Bickelhaupt, F. M.; Gisbergen, S. J. A. van; Fonseca Guerra, C.; Baerends, E. J.; Snijders, J. G.; Ziegler, T. *J. Comput. Chem.* **2001**, *22*, 931. Fonseca Guerra, C.; Snijders, J. G.; te Velde, G.; Baerends, E. J. *Theor. Chem. Acc.* **1998**, *99*, 391.
(26) Vosko, S. H.; Wilk, L.; Nusair, M. *Can. J. Phys.* **1980**, *58*, 1200.
(27) (a) Becke, A. D. *J. Chem. Phys.* **1986**, *84*, 4524. (b) Becke, A. D. *Phys. Rev.* **1988**, *A38*, 3098.
(28) (a) Perdew, J. P. *Phys. Rev.* **1986**, *84*, 4524. (b) Perdew, J. P. *Phys. Rev.* **1986**, *A34*, 7406.
(29) Snijders, J. G.; Baerends, E. J.; Vernooijs, P. *At. Data Nucl. Data Tables*, **1982**, *26*, 483. Vernooijs, P.; Snijders, J. G.; Baerends, E. J. *Slater Type Basis Functions for the Whole Periodic System*, Internal Report; Free University of Amsterdam: The Netherlands, 1981.
(30) *MAYER.* A program to calculate Mayer bond-order indices from the output of the electronic structure packages GAMESS, GAUSSIAN, and ADF, written by A. J. Bridgeman, University of Hull 2001. Available from the author on request.
(31) Haddon, R. C.; Scott, L. T. *Pure Appl. Chem.* **1986**, *58*, 137.
(32) Gunda, T. E. *Mol2Mol*, version 4.0; CompuChem Software Chemie: Niedernhall, Germany, 2001.
(33) (a) Haddon, R. C. *Science* **1993**, *261*, 1545. (b) Haddon, R. C. *J. Am. Chem. Soc.* **1990**, *112*, 3385. (c) Haddon, R. C. *Acc. Chem. Res.* **1988**, *21*, 243.
(34) Ioffe, I. N.; Boltalina, O. V.; Sidorov, L. N.; Dorn, H. C.; Stevenson, S.; Rice, G. *Fullerenes: Recent Advances in the Chemistry and Physics of Fullerenes and Related Materials*; Kadish, K. M., Ruoff, R. S., Eds., Electrochmical Society: Pennington, 2000 and references therein.
(35) Wang, L. S.; Alford, J. M.; Chai, Y. Diener, M.; Smalley, R. E. *Chem. Phys. Lett.* **1993**, *207*, 354.

described as C_{80}.[6−36] Again, it is interesting that the difference is caused by encapsulated species. In conclusion, the electron-attracting character of the TNT endohedral metallofullerenes compared with that of the free fullerenes suggests that the former are much less reactive toward nucleophiles after the TNT encapsulation.

Geometric Effect: Strength of the C−C Bonds. Mayer Bond Order (MBO) and Bond Lengths. The MBO[37] is a measure of the electron density of C−C bonds as a generalization of the Wiberg bond index.[38] The MBO is related to the number of shared electron pairs between the atoms and is calculated using the density and overlap matrixes. The MBO has proved to be an extremely useful, transparent, analytical, and interpretative tool for measuring the strength of a chemical bond.[39] If the involved atoms are the same, bond lengths follow the same trend as MBO; the higher the MBO, the shorter bond length. The MBO analysis finds 1.209 for the 6:6 C−C bonds and 1.194 for the 5:6 C−C bonds in the free I_h-C_{80}:**7** cage. To get some idea whether the relative differences are significant, the MBO must be compared with the C_{60} and C_{70} values. The MBO of the 6:6 C−C bond of C_{60} is computed to be 1.342 and the 6:6 Ca−Cb bond of C_{70} 1.334 (Supporting Information, Tables A.1 and A.3), whereas the 5:6 C−C bond of C_{60} is computed to be 1.136. A difference of 0.20 between the most reactive and the least in the C_{60} suggests that no significant difference exists between the two different C−C bonds in the free I_h-C_{80}:**7** cage. On the other hand, three main rules emerge after the TNT encapsulation unit inside the I_h-C_{80}:**7** cage: (1) MBOs do not change considerably except in the C−C bonds of the interacting region that directly faces the Sc atoms, (2) the highest MBOs are never found in those regions but in the regions at top and bottom of the TNT unit; (3) the range of MBO is amplified from 1.089 to 1.247 values for the different types of C−C bonds of the fullerene complex but keeping the similarities between 6:6 and 5:6 C−C bonds. The description (bond lengths, MBOs and pyramidalization angles) of all different types of C−C bonds for C_{2v}-$Sc_3N@C_{80}$:**7** (34 different sets of C−C bonds), C_3−$Sc_3N@C_{80}$:**1** (24) and C_s-$Sc_3N@C_{80}$:**2** (64) isomers are collated in Supporting Information (Tables A.6, A.7, and A.8).

Geometric Effect: Pyramidalization Angle of Carbons. The relationship between the local atomic structure and the chemical reactivity of fullerenes was characterized by Haddon using the pyramidalization angle of carbons (θ_p).[40] The pyramidalization angle is a simple quantitative measure of the local curvature and strain in carbon systems. The pyramidalization angle is obtained as $\theta_p = \theta_{\sigma\pi} - 90$. In POAV1[41] analysis, the $\theta_{\sigma\pi}$ (π-orbital axis vector) is introduced and defined as that vector that makes equal angles to the three σ-bonds at a conjugated carbon atom. For planar sp^2 carbons the $\theta_{\sigma\pi}$ is 90°, whereas for tetrahedral sp^3 carbons this angle is 109.47°. Consequently, the pyramidalization angle is 0° for sp^2 centers, 19.47° for sp^3 centers and 11.67° for C_{60}. There are other methods of calculating the pyramidalization but POAV1 is conceptually simple and widely used.[42] The corannulene 5:6 C−C bonds (***D*** type) are more highly pyramidalized (θ_p = 10.58°) than the 6:6 C−C bonds (***B*** type, θ_p = 9.62°) in the free I_h-C_{80}:**7**. Three important conclusions can be drawn from the pyramidalization angle analysis after the TNT encapsulation: (1) the changes are not severe except in the C−C bonds closest to the Sc atoms, which become the most pyramidalized; (2) the most pyramidalized C−C bonds are still the corannulene 5:6 C−C bonds; and (3) the highest pyramidalization angles, apart from C−C bonds connected to scandiums, are only found in the $Sc_3N@C_{80}$:**1** and **2** isomers. Unlike the two above-mentioned complexes, in the $Sc_3N@C_{80}$:**7** complex the Sc atoms face one C_6 ring and two C_5 rings, so none of the C−C bonds are pyramidalized in a particular way.

Combination of All Considerations: Prediction of the Most Reactive Sites of $Sc_3N@C_{80}$. According to the calculations, in the case of the free I_h-C_{80}:**7** the pyramidalization angle becomes the most important factor in determining the most reactive site since the MBOs are almost equal. So, the cycloaddition of 1,3-butadiene to the most pyramidalized 5:6 C−C bond (***D*** type) gives an isomer 16.1 kcal mol^{-1} more stable than the reaction toward the 6:6 C−C bond (***B*** type). After the TNT encapsulation and due to the loss of symmetry, the simplicity of the I_h-C_{80}:**7** fullerene cage with only two different C−C bonds is transformed to a huge variety of slightly different C−C bonds with a wide range of MBOs, pyramidalization angles, and C−C bond lengths (Tables A.8−A.10 in Supporting Information). However, TNT encapsulation presumably will not change the reactivity differences between the 6:6 and 5:6 C−C bonds because we have demonstrated in the previous sections that, in general, the encapsulation only provokes slightly geometric modifications in the characteristics of the C−C bonds, excepts in the carbon region where the Sc atoms are facing. In this region, the pyramidalization of the carbon atoms is extremely increased (∼13°), and simultaneously, the MBO (∼1.12) and C−C distances (∼1.47 Å) are markedly reduced; in consequence, this makes them not suitable for addition reactions. The rest of the 5:6 and 6:6 C−C bonds will keep a similar reactivity as in I_h-C_{80}:**7**, and thus, probably some of the 5:6 C−C with the highest MBO and pyramidalization angle will still be the most reactive site.

[4 + 2] Cycloaddition of 1,3-Butadiene on $Sc_3N@C_{80}$. Once the various factors affecting the exohedral reactivity were analyzed, we took the predicted most reactive sites to perform a cycloaddition reaction of 1,3-butadiene on the $Sc_3N@C_{80}$ isomers. Notice that the experimental stoichiometry of the Diels−Alder cycloadduct $Sc_3N@C_{80}$-$C_8H_6(OCH_3)_2$ was modeled as $Sc_3N@C_{80}$-C_4H_6.

The most reactive 5:6 C−C bonds for $Sc_3N@C_{80}$ isomers, according to the MBO, are the C44−C64 bonds for $Sc_3N@C_{80}$:**6** isomer, the C1−C2 and C17−C37 bonds for $Sc_3N@C_{80}$:**1** isomer, and the C1−C2 and C46−C65 bonds for $Sc_3N@C_{80}$:**2** isomer. Calculations corroborate that the most reactive site coincides with that found experimentally: the formation of an adduct in the corannulene 5:6 C1−C2 bond of the $Sc_3N@C_{80}$:**2** isomer, although other 5:6 C−C bonds show similar reactivity (0.5−5.3 kcal mol^{-1}). So, for instance, the reaction toward the 5:6 C1−C2 bond of the $Sc_3N@C_{80}$:**1** isomer gives a similar

(36) Iiduka, Y.; Ikenaga, O.; Sakuraba, A.; Wakahara, T.; Tsuchiya, T.; Maeda, Y.; Nakahodo, T.; Akasaka, T.; Kako, M.; Mizorogi, N.; Nagase, S. *J. Am. Chem. Soc.* **2005**, *27*, 9956.

(37) (a) Mayer, I. *Chem. Phys. Lett.* **1983**, *97*, 270. (b) Mayer, I. *J. Quantum Chem.* **1984**, *26*, 151.

(38) Wiberg, K. A. *Tetrahedron* **1968**, *24*, 1083.

(39) Bridgeman, A. J.; Cavigliasso, G. *Faraday Discuss.* **2003**, *124*, 239.

(40) (a) Haddon, R. C.; Scott, L. T. *Pure Appl. Chem.* **1986**, *58*, 137. (b) Haddon, R. C. *J. Am. Chem. Soc.* **1986**, *108*, 2837. (c) Haddon, R. C.; Chow, S. Y. *J. Am. Chem. Soc.* **1998**, *120*, 10494.

(41) Haddon, R. C. *Acc. Chem. Res.* **1988**, *21*, 243.

(42) (a) Rabideau, P. W.; Sygula, A. *Acc. Chem. Res.* **1996**, *29*, 235. (b) Abdourazak, A. H.; Marcinow, Z.; Sygula, A.; Sygula, R.; Rabideau, P. W. *J. Am. Chem. Soc.* **1995**, *117*, 6410.

TABLE 1. Geometric Properties and Relative Energies for $Sc_3N@C_{80}$-C_4H_6 and C_{80}-C_4H_6 Isomers[a]

					$Sc_3N@C_{80}/C_{80}$			$Sc_3N@C_{80}$-C_4H_6/C_{80}-C_4H_6	
type[b]	type	isomer	C−C bond	symmetry	bond length	initial θ_p[c]	MBO	final θ_p[c]	relative energy
I_h-C_{80}:**7**	5:6			C_s	1.438	10.58	1.194	19.91	0.0[e]
	6:6			C_1	1.428	9.62	1.209	18.74	16.1
$Sc_3N@C_{80}$	5:6	**2**	1,2	C_s	1.430	11.02	1.233	20.68	0.0[d]
			46,65	C_1	1.433	10.70	1.226	20.08	5.3
		1	1,2	C_s	1.432	10.90	1.228	20.70	0.5
			17,37	C_1	1.437	10.54	1.209	19.81	13.0
		7	1,2	C_s	1.439	10.43	1.192	20.86	3.6
			44,64	C_1	1.434	10.55	1.223	20.85	3.7
		3	1,2	C_s	1.432	10.93	1.231	20.68	1.2
		5	1,2	C_s	1.432	10.97	1.231	20.66	3.6
		4	1,2	C_1	1.441	10.09	1.188	20.59	6.5
		6	1,2	C_1	1.448	9.76	1.162	20.34	11.8
	6:6	**2**	9,10	C_1	1.422	9.72	1.246	18.97	11.1
			66,67	C_1	1.421	9.67	1.242	18.85	12.1
		1	9,10	C_1	1.423	9.63	1.245	19.05	10.7
			26,27	C_1	1.424	9.82	1.224	18.84	16.6
		7	36,47	C_1	1.427	9.37	1.200	19.66	25.1

[a] Bond lengths in Å, angles in deg, and energies in kcal mol^{-1}. [b] See Figure 2 for a graphical representation of the different types of C−C bonds. [c] Pyramidalization angle (θ_p) for the carbons attached to the diene. [d] Reaction energy of $Sc_3N@C_{80}$:**2** + 1,3-butadiene → $Sc_3N@C_{80}$-C_4H_6 is computed to be −12.3 kcal mol^{-1}. [e] Reaction energy of I_h-C_{80}:**7** + 1,3-butadiene → C_{80}-C_4H_6 is computed to be −24.0 kcal mol^{-1}.

stability, +0.5 kcal mol^{-1}, thus indicating that a restricted movement of the TNT unit is still possible and not only one isomer of $Sc_3N@C_{80}$ is present. These results also corroborate the fact that a small degree of disorder in the positions of the scandiums ions was found in the X-ray determination. The relative energies, MBOs, and some geometrical parameters (bond lengths, initial θ_p, and final θ_p) of the cycloaddition adducts are listed in Table 1. Finally, we computed the cycloaddition of 1,3-butadiene on the C1−C2 bond of the rest of $Sc_3N@C_{80}$ isomers (**3**, **4**, **5**, and **6**) to investigate whether Sc_3N can freely rotate inside the carbon cage after the cycloaddition reaction or whether, on the other hand, the encapsulation can help to fix the TNT unit. The main conclusion is that movement is only slightly more hindered after the cycloaddition of the diene, but the TNT can still rotate. The relative energies of the Sc_3N motion inside C_{80}−C_4H_6 are slightly higher than those found for the Sc_3N motion inside the I_h-C_{80}:**7**. Only isomer **6** decreases the relative energy from 5.3 to 3.6 kcal mol^{-1}, whereas the other isomers increase the relative energies, for instance, isomer **7** from 1.4 to 6.5 kcal mol^{-1} (Figure 3 and Table 1). We also calculated the reactivity of the two most reactive 6:6 C−C bonds of the $Sc_3N@C_{80}$:**1** isomer (C9−C10 and C26−C27) and $Sc_3N@C_{80}$:**2** isomer (C9−C10 and C66−C67) and the most reactive of $Sc_3N@C_{80}$:**7** isomer (C36−C47) according to the MBO. All of them are at least 10 kcal mol^{-1} less stable than the reaction toward the 5:6 C1−C2 bond of $Sc_3N@C_{80}$:**2** isomer. So, the calculations still indicate the high regioselectivity in the 5:6 C−C bond on the cycloaddition reaction of the $Sc_3N@C_{80}$ carbon surface, although the energy difference between both types of C−C bonds has reduced from 16.1 for the free I_h-C_{80}:**7** to 10.7 kcal mol^{-1} for the $Sc_3N@C_{80}$.

To sum up, 5:6 C−C bonds still are the most reactive sites (0.0−5.3 kcal mol^{-1}) against 6:6 C−C bonds (10.7−25.1 kcal mol^{-1}) after the TNT encapsulation. These results are in pronounced contrast to those observed for $Y_3N@C_{80}$, for which very recently reported derivatives (pyrrolidine monoadduct and diethyl malonate monoadduct) add completely regioselectively to 6:6 double bonds.[43] Preliminary results point at kinetic considerations to explain it. On the other hand, TNT rotation is more hindered but possible, although some relative positions between the addend and the TNT unit especially become much less stable, for instance, C17−C37 in $Sc_3N@C_{80}$:**1** and C1−C2 in $Sc_3N@C_{80}$:**6** isomer with a relative energy of 13.0 and 11.8 kcal mol^{-1}, respectively. This lack of stabilization of some 5:6 C−C bonds can be explained from geometric considerations during the pyramidalization of the carbons in the cycloaddition. The correlation between the final pyramidalization angle (final θ_p) in the cycloaddition adducts and the relative energies indicate that if both fragments are to be bound efficiently, the pyramidalization angle must be high. So, the isomers that more facilitate the pyramidalization of carbons will tend to be more stable. For the less reactive 5:6 C−C bonds, the lowest final pyramidalization angle is 19.81° for C17−C37 of $Sc_3N@C_{80}$:**1** and 20.34° for C1−C2 of $Sc_3N@C_{80}$:**6**. Also, the final pyramidalization of the less reactive 6:6 C−C bonds (ca. 19°) never arrives to the values of the most reactive 5:6 C−C bonds (ca. 20°).

For the most stable cycloaddition adduct, the C1−C2 distance (1.632 Å) is considerably longer than the average C1−C2 distance at the unaltered site (1.430 Å). The experimental value was 1.626 Å. The carbons C1 and C2 are pulled away from the center up to a maximum pyramidalization angle of 20.7° (experimental value of 21°). The average of the five Sc−C contacts is computed to be 2.283 Å, quite close to the experimental value of 2.272 Å and similar to the computed value for the free $Sc_3N@C_{80}$:**2** isomer (2.276 Å). The Sc_3N unit is planar and positioned well away from the site of external modification. The mean Sc−N distances (2.016 Å calculated and 2.027 Å measured) are also slightly longer than those in the free $Sc_3N@C_{80}$:**2** (2.012 Å). Finally, it should be noted that the cycloaddition increases the cage radius again, from 4.118 Å for $Sc_3N@C_{80}$:**2** to 4.122 Å for $Sc_3N@C_{80}$-C_4H_6. To sum up, the computed geometry of the functionalized structure of $Sc_3N@C_{80}$ matches perfectly the experimental geometry proposed by Balch and co-workers.[15] The above-mentioned structures are drawn in Figure 4 and some geometrical parameters are listed in Table 2.

(43) Cardona, C. M.; Kitaygorodskiy, A.; Echegoyen, L. *J. Am. Chem. Soc.* **2005**, *127*, 10449.

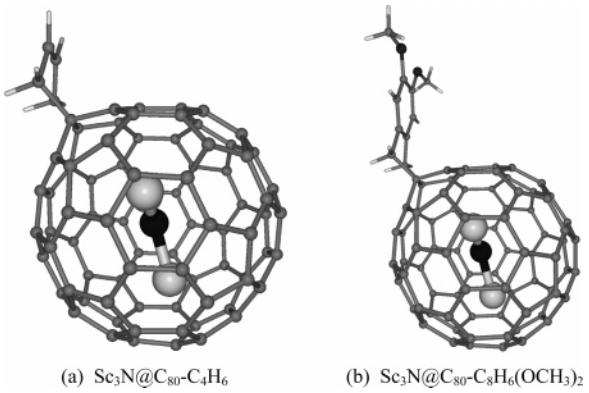

(a) $Sc_3N@C_{80}$-C_4H_6 (b) $Sc_3N@C_{80}$-$C_8H_6(OCH_3)_2$

FIGURE 4. Structures for the most stable $Sc_3N@C_{80}$-C_4H_6 isomer (a) and for the X-ray of $Sc_3N@C_{80}$-$C_8H_6(OCH_3)_2$ (b).

TABLE 2. Crucial Geometric Parameters That Change during the Derivatitzation via a [4 + 2] Cycloaddition Reaction on $Sc_3N@C_{80}$:2 Isomer[a]

	$Sc_3N@C_{80}$:**12**[b]	$Sc_3N@C_{80}$-C_4H_6 [b]	$Sc_3N@C_{80}$-$C_8H_6(OCH_3)_2$ [c]
Sc−N bond lengths[d]	2.008−2.019	2.010−2.019	2.021−2.032
Sc−C bond lengths[e]	2.258	2.268	2.244
cage radius[f]	4.118	4.122	4.098
C1−C2 θ_p	11.02	20.68	21
C1−C2 bond lengths	1.430	1.632	1.626

[a] Distances in Å and angles in deg. [b] DFT calculations. [c] X-ray data from ref 15. [d] Range of Sc−N bond lengths. [e] Contact distances between Sc and the nearest neighbor carbons. [f] Cage radius of the free I_h-C_{80}:**7** was computed to be 4.103 Å.

TABLE 3. [4 + 2] Cycloaddition Energy of 1,3-Butadiene on the Two Types of C−C Bonds for Several Dienophiles[a]

dienophile	type of C−C	energy reaction	type of C−C	energy reaction
I_h-C_{60}:**1**	6:6, ***A***	−16.7	5:6, ***D***	−0.6
I_h-C_{80}:**7**	5:6, ***D***	−24.0	6:6, ***B***	−7.9
$Sc_3N@C_{80}$	5:6, ***D***	−12.3	6:6, ***B***	−1.6
D_{3h}-$Sc_3N@C_{78}$	6:6, ***B***	−8.6	6:6, ***A***	−3.5
ethylene [b]		−38.9		

[a] Energies in kcal mol^{-1}. [b] Experimental value of −40.5 kcal mol^{-1}

The energy involved in the addition reaction to the free I_h-C_{80}:**7** is almost twice that of the addition reaction to $Sc_3N@C_{80}$:**2**, which corroborates the prediction of the decrease in the exohedral reactivity of TNT endohedral metallofullerenes. We calculated the addition reaction between $Sc_3N@C_{80}$:**2** and 1,3-butadiene, which was −12.3 kcal mol^{-1}, and the reaction energy between I_h-C_{80}:7 and 1,3-butadiene, which was −24.0 kcal mol^{-1}, see Table 3. However, it is important to notice that these TNT endohedral metallofullerenes still continue to be similarly reactive as the free pyracylene 6:6 bond (***A*** type) of the C_{60}, since the reaction energy is calculated to be only −16.7 kcal·mol^{-1}. The present level of computation is capable of reproducing accurately the reaction energy, which was calculated to be −38.9 kcal·mol^{-1} for the cycloaddition reaction of 1,3-butadiene on the ethylene, whereas the experimental value was found to be very close, −40.5 kcal·mol^{-1}.[44]

Clues about [4 + 2] Cycloaddition of 1,3-Butadiene on $Sc_3N@C_k$ (k = 68, 78). The significant results obtained above in predicting the most reactive exohedral sites of $Sc_3N@C_{80}$ prompted us to investigate the [4 + 2] cycloaddition to other known TNT endohedral metallofullerenes: D_3-$Sc_3N@C_{68}$ and D_{3h}-$Sc_3N@C_{78}$. The task seemed easier because there is only one possible isomer for these TNT endohedral complexes and consequently the TNT cannot rotate freely. We used the same strategy. First, we located the highest MBO with a high pyramidalization angle in the TNT endohedral metallofullerenes of D_3-C_{68}:**6140** and $D_{3h'}$-C_{78}:**5**. Table 4 lists the bond lengths, the pyramidalization angles, and the MBOs of the different sets of C−C bonds of the $D_{3h'}$-C_{78}:**5**, D_{3h}-$Sc_3N@C_{78}$, D_3-C_{68}:**6140**, and D_3-$Sc_3N@C_{68}$. The reactivity of these TNT endohedral metallofullerenes is also predicted to be reduced as a result of the lower electron-attracting character of the endohedral molecules compared to that of free fullerenes. The electron affinity decreases from 3.49 to 2.55 eV during the TNT encapsulation inside the $D_{3h'}$-C_{78}:**5** and from 3.71 to 2.47 eV for D_3-C_{68}:**6140**.[19] From the geometric point of view, as was expected, the effect of the TNT encapsulation is similar to that described by the I_h-C_{80}:**7** fullerene: the main characteristics of the C−C bonds are maintained except in the C−C bonds near the scandiums where the MBO decreases and the pyramidalization angle increases significantly. Systematic description (bond lengths, pyramidalization angle, and MBO) of all different types of C−C bonds of D_3-C_{68}:**6140**, D_3-$Sc_3N@C_{68}$, $D_{3h'}$-C_{78}:**5**, and D_{3h}-$Sc_3N@C_{78}$ can be found in Tables A.2 and A.4 and Figures A.2 and A.4 in Supporting Information.

The free $D_{3h'}$-C_{78}:**5** isomer has 13 distinct sets of C−C bonds and it is one of the fullerenes in which the four possible types of C−C bonds for IPR fullerenes are present, ***A***−***D*** types in Figure 2. All C−C bonds of the $D_{3h'}$-C_{78}:**5** isomer involve 6:6 or 5:6 ring junctions. There are several kinds of 6:6 C−C bonds, which range in length from 1.372 to 1.469 Å. The shortest ones appear in the pyracylene patches. The 5:6 C−C bonds have an average length of 1.44 Å. Two distinct sets of pyracylene C−C bonds are expected to be the most reactive sites for the free $D_{3h'}$-C_{78}:**5**: the C1−C2 and C27−C28 bonds. Both C−C bonds have a markedly high MBO (1.392 and 1.373, respectively), which predicts regioselectivity across cycloadditions reaction (Table 4). These C−C bonds have MBOs even higher than those of the 6:6 C−C bonds in C_{60} and the Ca−Cb in C_{70}. After Sc_3N encapsulation (scandiums are facing the set of C27−C28 bonds), only the three distinct C1−C2, C7−C21, and C8−C24 bonds appear as the most reactive sites, the others being completely discarded because of their lower MBOs. The fourth highest MBO (C23−C44) is 0.06 lower than the third one (C1−C2). Notice that the C27−C28 bond had a high double bond character (MBO = 1.373), but after the coordination of the scandium atoms this bond is completely deactivated (MBO = 1.086). On the other hand, the C8−C24 bond is activated after the TNT encapsulation. Figure 5 shows the change of the reactive regions when the TNT is encapsulated into the $D_{3h'}$-C_{78}:**5** fullerene. Notice that the easy panorama of the predicted regioselectivity in the D_{3h}-C_{78}:**5** and D_{3h}-$Sc_3N@C_{78}$ differs completely of the complexity found in the I_h-C_{80}:**7** and their TNT endohedral metallofullerene. However, selective calculations are necessary to determine the most reactive site because the 6:6 C7−C21 bond and the C8−C24 bond have the highest MBO of 1.271 and 1.280, respectively but a low pyramidalization angle of ca. 10°, whereas the set of C1−C2 bonds also has a high MBO (1.267) with a considerable pyramidalization angle of 11.28°. The ^{13}C and ^{1}H NMR data of the monoadduct support the idea

(44) Chikama, A.; Fueno, H.; Fujimoto, H. *J. Phys. Chem.* **1995**, *99*, 8541.

TABLE 4. Change of Characteristics of the Six Most Reactive C−C Bonds for D_{3h}-C_{78}:5 (Initial)/D_{3h}-$Sc_3N@C_{78}$ (Final) and D_3-C_{68}:6140 (Initial)/D_3-$Sc_3N@C_{68}$ (Final) Fullerenes[a]

	C−C bond[b]	type[c]	initial bond length	final bond length	initial θ_p[d]	final θ_p[d]	initial MBO[e]	final MBO[e]
D_{3h}-C_{78}:**5**/D_{3h}-$Sc_3N@C_{78}$	8,24	***B***	1.424	1.403	9.48	10.05	1.214	1.280[f]
	7,21	***B***	1.419	1.429	9.63	9.51	1.283	1.271[f]
	1,2	***A***	1.392	1.403	11.67	11.28	1.392	1.267[f]
	23,44	***D***	1.470	1.427	10.31	9.20	1.090	1.208
	27,28[g]	***A***	1.372	1.441	10.47	13.88	1.373	1.086
D_3-C_{68}:**6140**/D_3-$Sc_3N@C_{68}$	14,24	***B***	1.429	1.437	9.71	9.97	1.252	1.219
	2,13	***D***	1.449	1.439	10.14	10.35	1.159	1.218
	1,2	***B***	1.431	1.432	9.58	9.55	1.215	1.201
	2,3	***D***	1.433	1.439	10.90	10.69	1.210	1.199
	15,27	***A***	1.396	1.416	11.52	11.56	1.266	1.152
	23,24	***B***	1.418	1.454	9.93	9.60	1.257	1.123

[a] Bond lengths in Å and pyramidalization angle deg. The complete list of the 13 different sets of C−C bonds for D_{3h}-C_{78}:**5**/D_{3h}-$Sc_3N@C_{78}$ and the 18 for D_3-C_{68}:**6140**/D_3-$Sc_3N@C_{68}$ are in Tables A.4 and A.2 in Supporting Information, respectively. [b] See Figure 5 for the systematic numeric system of D_{3h}-C_{78}:**5**, extracted from ref 16. See Figure 6 for the localization of the most reactive C−C bonds of the D_3-C_{68}:**6140** and D_3-$Sc_3N@C_{68}$. For a complete numbering system of D_3-C_{68}:**6140** see Figure A.2 in Supporting Information. [c] See Figure 2 for a graphical representation of the different types of C−C bonds (***A***−***D***). [d] Average pyramidalization angle (θ_p) of each carbon atom in the C−C bond. [e] Mayer bond order (MBO). [f] The reaction energy of the cycloaddition of 1,3-butadiene was calculated to be −8.6 kcal mol^{-1} for C8−C24, −6.0 kcal mol^{-1} for C7−C21, and −3.5 kcal mol^{-1} for C1−C2 bond. [g] Sc atoms are facing endohedrally this site.

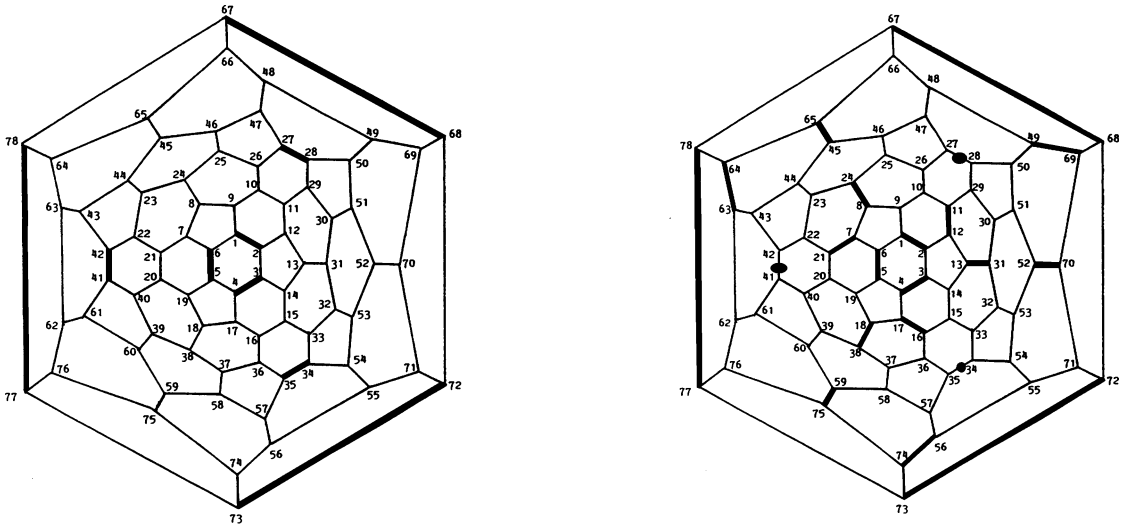

(a) $D_{3h'}$-C_{78}:**5** (b) D_{3h}-$Sc_3N@C_{78}$

FIGURE 5. The most reactive exohedral sites for $D_{3h'}$-C_{78}:**5** (a) and $Sc_3N@C_{78}$ (b) drawn in a Schlegel diagram. Sc atoms are facing the fullerene surface in the circle positions in (b). The set of C1−C2 and C27−C28 bonds have been marked (bold lines) for the free $D_{3h'}$-C_{78}:**5** in (a); the set of C8−C24, C7−C21, and C1−C2 bonds for D_{3h}-$Sc_3N@C_{78}$ in (b). The C−C bonds equivalent to C1−C2 are C3−C4, C5−C6, C67−C68, C72−C73, and C78−C79; those equivalent to C27−C28 are C34−C35 and C41−C42; those equivalent to C8−C24 are C13−C31, C18−C38, C45−C65, C52−C70, C59−C75; and those equivalent to C7−C21 are C11−C12, C16−C17, C49−C69, C56−C74, and C63−C64. The systematic numbering system is taken from ref 16.

that addend addition takes place at an asymmetric site on the $D_{3h'}$-C_{78}:**5**. So we can discard the reaction toward the C1−C2 bond because these would give symmetric structures and thus the C7−C21 and C8−C24 seem to be the reactive sites. Calculations confirm that both asymmetric sites give higher reaction energy, −8.6 and −6.0 kcal mol^{-1} for C8−C24 and C7−C21, respectively, whereas the reaction toward the C1−C2 bond is 5.1 kcal·mol^{-1} less reactive than the reaction toward the C8−C24 bond. Notice as well, that the TNT of $D_{3h'}$-C_{78}:**5** fullerene is predicted to be less reactive than the analogous of I_h-C_{80}:**7** toward the cycloaddition of 1,3-butadiene.

The non-IPR D_3-C_{68}:**6140** fullerene is significantly different from the other mentioned fullerenes since it has 5:5 ring junctions (***E*** type). The distance of this kind of C−C bond is computed to be 1.436 Å. As in the $D_{3h'}$-C_{78}:**5** cage, reactive pyracylene C−C bonds are also found in this isomer of C_{68}. The computed average distance for this type of C−C bond is 1.396 Å, similar to the 6:6 C−C bond lengths in C_{60} and $D_{3h'}$-C_{78}:**5**. $D_{3h'}$-C_{78}:**5** and I_h-C_{80}:**7** are spherical, so all carbons are approximately at the same distance from the center: the cage radius is 4.052 and 4.103 Å, respectively. Nevertheless, the cage radius of D_3-C_{68}:**6140** is not only considerably shorter (3.783 Å) but also distorted, with only one plane that can encapsulate the TNT unit guest; see Figure 1c. In this plane, the scandiums are directly connected to 5:5 ring junctions and the N-carbon cage distances are similar to those found in $D_{3h'}$-C_{78}:**5** and I_h-C_{80}:**7** cages. A first general view of the characteristics of all different sets of C−C bonds of the free D_3-C_{68}:**6140** and the $Sc_3N@C_{68}$ shows that no C−C bond has a significant high and different MBO to predict it as the most reactive; see Table 4. So D_3-C_{68}:**6140** fullerene is more similar to the I_h-C_{80}:**7** fullerene than to the D_{3h}-C_{78}:**5** in this aspect. According to MBO analysis

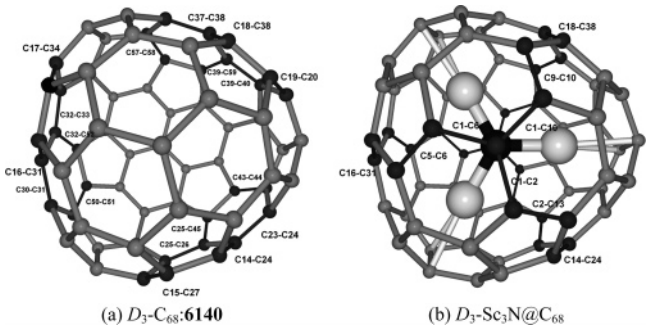

(a) D_3-C_{68}:**6140** (b) D_3-$Sc_3N@C_{68}$

FIGURE 6. The three most reactive exohedral sites for D_3-C_{68}:**6140** (a) and D_3-$Sc_3N@C_{68}$ (b). The set of C15−C27, C23−C24, and C14−C24 bonds have been marked (bold lines) for the free D_3-C_{68}:**6140** in (a); the set C14−C24, C2−C13, and C1−C2 bonds for D_3-$Sc_3N@C_{68}$ are in (b). The C−C bonds equivalent to C15−C27 are C17−C34, C19−C20, C43−C44, C50−C51, and C57−C58; those equivalent to C23−C24 are C25−C26, C30−C31, C32−C33, C37−C38 and C39−C40; those equivalent to C14−C24 are C18−C38, C16−C31,C25−C45, C32−C52 and C39−C59; those equivalent to C2−C13 are C5−C6, C9−C10, C46−C63, C53−C65, and C60−C67; those equivalent to C1−C2 are C1−C6, C1−C10, C63−C68, C65−C68, and C67−C68.

the most reactive sites in the non-IPR D_3-C_{68}:**6140** fullerene could be the 6:6 C−C bonds: C15−C27, C23−C24, or C14−C24 (Table 4 and Figure 6). If we assume that the 6:6 pyracylene C−C bonds (***A*** type) are the most reactive sites, then the C15−C27 could be the preferred site. When the Sc_3N is encapsulated, the most reactive sites could move to the C14−C24, C2−C13, or C1−C2 bonds, but if the rule of the preference for the corannulene 5:6 C−C bonds is accomplished, the C2−C13 should be the most reactive site. Figure 6 shows how the most reactive C−C sites are moved from the Sc_3N plane to the top of the fullerene cage. It would be also interesting to know the reactivity of the 5:5 C21−C42 bond, although according to the MBO it is predicted to be quite low.

Conclusions

$Sc_3N@C_{80}$ complex has already been exohedrally functionalized via a Diels−Alder cycloaddition of the 6,7-dimethoxyisochroman-3-one. The study of the electronic and geometric effects of the TNT encapsulation has been crucial for predicting the exohedral reactivity of the cage. Moreover, DFT calculations were carried out on the series of [4 + 2] cycloaddition reactions of 1,3 butadiene on $Sc_3N@C_{80}$ isomers in order to find the most reactive C−C bond. Since the Diels−Alder reactions are facilitated by electron-withdrawing dienophiles, the TNT endohedral metallofullerenes are less reactive than the free fullerene cages due to their lower electron affinities, ca. 1 eV. This is a consequence of the previous six electron transfer from the TNT unit to the carbon cage described as $Sc_3N^{6+}@C_k^{6-}$ (k = 68, 78, and 80). Apart from the electronic effect of the TNT encapsulation, there is also a geometric effect on the double bond character and pyramidalization angle of the C−C bonds. In general, all C−C bonds retain their main characteristics (bond lengths, bond order, and pyramidalization) after the encapsulation of a TNT unit, except those C−C bonds of the carbon region nearer to the scandium atoms, which become completely deactivated as the result of an extremely low double bond character. In the case of I_h-C_{80}:**7** and $Sc_3N@C_{80}$, the most pyramidalized corannulene 5:6 C−C bonds are more preferred sites than the 6:6 C−C bonds. However, the TNT encapsulation produces a decrease of the difference between both types (decrease of regioselectivity), 16.1 kcal mol^{-1} in the former and only 10.1 kcal mol^{-1} in the latter. Specifically, the cycloaddition occurs on the corannulene 5:6 C1−C2 bond in a TNT orientation corresponding to $Sc_3N@C_{80}$:**2** isomer, which coincides with the experimental cycloaddition product: $Sc_3N@C_{80}$-$C_8H_6(OCH_3)_2$. The reaction energy for this site was calculated to be −12.3 kcal mol^{-1}, 11.7 kcal mol^{-1} lower than the hypothetical reaction to the corresponding site of the free fullerene. Once the dienophile is fixed in a 5:6 C−C bond, DFT calculations corroborate a partial random circular motion of the TNT units, although some TNT orientations are calculated to be particularly quite unfavorable. TNT rotation gives the formation of a high number of hypothetical isomers and thus a high number of slightly different C−C bonds, but none of the isomers breaks the rule for the preference of the corannulene 5:6 C−C bonds. In the case of $Sc_3N@C_{78}$, the cycloaddition of 1,3-butadiene seems less favorable than in the $Sc_3N@C_{80}$. Unlike $Sc_3N@C_{80}$, there is only one TNT orientation, and the double bond character and the pyramidalization angle analysis emphasize just a few possible isomers as the most reactive ones. Calculations also confirm the experimental evidence that the most reactive site corresponds to an asymmetric site: the 6:6 C8−C24 bond. For D_3-C_{68}:**6140** and $Sc_3N@C_{68}$ no clear C−C bond emerges from the analysis for the most reactive and calculations will be required. To sum up, TNT encapsulation is a new tool for the control of regioselectivity in the addition reactions to fullerenes: it reduces the final reaction energy in relation to the free cage but does not change the geometric characteristics in the C−C bonds in regards to the free cages and thus their reactivity, except in those C−C nearer to the Sc atoms, which are completely deactivated.

Acknowledgment. This work was supported by the spanish MCyT (Ministry of Science and Technology) (BQU2002-04110-C02-02), by the DURSI of the Generalitat de Catalunya (SGR01-00315), and by the ICIQ (Institute of Chemical Research of Catalonia) Foundation.

Supporting Information Available: Systematic description (bond lengths, pyramidalization angle, and Mayer bond order) of all different types of C−C bonds of I_h-C_{60}:**1**, D_3-C_{68}:**6140**, D_3-$Sc_3N@C_{68}$, D_{5h}-C_{70}:**1**, $D_{3h'}$-C_{78}:**5**, D_{3h}-$Sc_3N@C_{78}$, I_h-C_{80}:**7**, C_{2v}-$Sc_3N@C_{80}$:**6**, C_{3v}-$Sc_3N@C_{80}$:**11**, and C_s-$Sc_3N@C_{80}$:**12** fullerenes; description tables accompanied by the corresponding Schlegel diagrams showing the numbering system and the geometrical structures with the localization of the C−C bonds; Cartesian coordinates and binding energy of the most representative structures considered in this study. This material is available free of charge via the Internet at http://pubs.acs.org.

JO051665S